Catalytic synthesis of carbon nanotubes on clay minerals

D. Gournis[a], M.A. Karakassides[a], T. Bakas[b], N. Boukos[c], D. Petridis[c,*]

[a]*Department of Materials Science and Engineering, University of Ioannina, GR-45110 Ioannina, Greece*
[b]*Department of Physics, University of Ioannina, GR-45110 Ioannina, Greece*
[c]*Institute of Materials Science, NCSR 'DEMOKRITOS', Ag. Paraskevi Attikis, GR-153 10 Athens, Greece*

Abstract

Novel clay–carbon tube composites were synthesized by catalytic decomposition of acetylene over iron-catalyst centers supported on montmorillonite surfaces by ion-exchange. TEM and SEM micrographs show the growth of carbon tubes rooted to the clay surfaces, while the iron-nanoparticles (which catalyze the formation of carbon-nanotubes) are detected and characterized by Mössbauer spectroscopy, mainly as ferromagnetic cementite (Fe_3C). In the hybrid materials the clay retains its exchange properties making possible the preparation of clay–carbon nanotube derivatives that are valuable for various technological applications.
© 2002 Elsevier Science Ltd. All rights reserved.

1. Introduction

Carbon nanotubes possess important properties derived from a combination of unique dimensional, structural and topological features [1–3]. In particular, electronic conductive or semiconductive behavior, excellent mechanical strength, stiffness and elasticity, low density, high thermal conductivity, open pipe framework and relative chemical inertness render carbon nanotubes outstanding materials for various potential technological applications including carbon tube electronics [4–7], light sources [7], light-weight but high-strength polymer composites [8,9], nanoprobes in high-resolution imaging [10], nanoelectrodes [11] and hydrogen reservoirs [12]. Prioritizing the needs for these challenges is the fabrication of well-defined and organized arrays of nanotubes. In this direction intensive research has yielded fruitful results and carbon nanotubes are presently prepared in sufficient quantities. Chemical routes to single-walled or multiple-walled carbon tubes rely mainly on metal particle (Fe, Co, Ni) catalyzed decomposition of hydrocarbon gases (methane, ethane, ethylene, acetylene). In addition, metal cations and metal

oxide centers embedded in solid supports promote effectively the synthesis of carbon nanotubes. Solid supports already employed comprise zeolites [13,14], mesoporous silica [15], silica [14,15], alumina [16] and graphite [14,17].

In this work we wish to report the use of aluminosilicate smectite clay as an alternative substrate for immobilizing the catalytic metal centers in the synthesis of carbon nanotubes. Owing to the unique swelling, ion-exchange and intercalation properties smectite clays can be easily, uniformly and reproducibly loaded with metal cations or oligonuclear metal oxide clusters that can function as catalysts in the growth of carbon nanotubes. In addition, carbon nanotubes rooted on smectite layers are particularly attractive for polymer reinforcing applications. Recent advances in clay–polymer composites [18–20] have established that small amounts of smectite clays dispersed in a polymer mass give composites with outstanding mechanical, thermal, optical and other properties that increase their technological value. In this frame, one would expect that the combined action of clay–carbon nanotubes in polymer matrixes would provide outstanding functionalities to the resulting composite materials. Pursuit of this goal imposes not only the need for an efficient method to produce clay–carbon nanotube hybrids, but also finding effective ways to disperse these hybrids in a polymer mass. In the present study, clay–carbon nanotubes were efficiently

*Corresponding author. Tel.: +30-10-650-3343; fax: +30-10-651-9430.

E-mail address: dpetrid@ims.demokritos.gr (D. Petridis).

synthesized by the catalytic decomposition of acetylene at 700 °C over an iron–clay catalyst.

2. Experimental

The clay used was a sodium-montmorillonite (Zenith-N) from the island Milos, Greece, with particles ≤ 2 μm, obtained by the Silver and Barytine Co. It was purified by well-established procedures in clay science. The structural formula for Zenith as determined from chemical analysis [21] is:

$$Na_{0.92}[Si_{7.75}Al_{0.25}]\{Al_{3.21}Mg_{0.69}Fe^{III}_{0.02}Fe^{II}_{0.03}Ti_{0.05}\}O_{20}(OH)_4$$
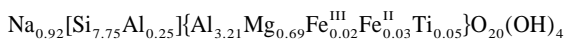
and its cation-exchange capacity (CEC) measured by the cobalt method is 80.2 mequiv/100 g clay. A 1 wt% clay suspension was reacted with aliquots of a 0.1 N $FeCl_3 \cdot 6H_2O$ aqueous solution such that the ratio $[FeCl_3]/[clay]$ was 5. After stirring for 3 h the clay-catalyst was washed well with water, separated by centrifugation, dried and finally calcined at 450 °C for 4.5 h. The synthesis of nanotubes was carried out on 50 mg catalyst in a fixed-bed flow reactor at 700 °C which was fed with a gas mixture of 8 ml/min acetylene (Linde) and 85 ml/min argon (Linde). The reaction was completed within 40 min and the carbon yield deposited was 192.5%, based on the mass of catalyst employed [14]. This yield is similar with that from iron–silica catalysts (184.0%), prepared by the ion-adsorption precipitation method, while other iron catalysts, such as Fe/graphite, Fe/Zeolite-X, Fe/ZSM-5 and Fe/silica, prepared by the impregnation method, give lower yield of carbon nanotubes [14]. Crude samples synthesized by the present process contained mostly multi-walled carbon nanotubes, and also amorphous carbon and possibly polyhedral carbon nanoparticles. When the clay–carbon nanotubes were intended as host materials for the intercalation of cationic surfactants, oxidation with potassium permanganate in acidic solution was necessary in order to remove the amorphous carbon from the nanotubes [22].

The intercalation of trimethylhexadecylammonium cations in a clay–carbon nanotube sample was achieved by reacting a 1 wt% aqueous clay–carbon nanotube suspension with aliquots from an aqueous ammonium salt solution such as the ratio $R = [salt]/[clay]$ was 1.5. After stirring for 3 h, the solid was washed twice with water, separated by centrifugation and air-dried by spreading on a glass plate. For the intercalation of triethylamine, vapors of the amine were allowed to contact the clay-nanotube composite for 24 h at 60 °C in a closed container.

Transmission electron microscopy observations were carried out with a Philips CM20 TEM operating at 200 kV, while a Philips 515 SEM operating at 30 kV was used to examine the formation of the tubes on the clay surfaces. Mössbauer measurements were carried out with a conventional constant acceleration spectrometer equipped with a $^{57}Co(Rh)$ source, calibrated with α-Fe and isomer shift values are reported relative to this. The spectra, recorded at liquid nitrogen temperature, were fitted on a PC with a least squares minimization procedure assuming Lorentzian line shapes. X-ray powder diffraction data were collected on a D8 Advance Bruker diffractometer by using Cu Kα (40 kV, 40 mA) radiation and a secondary beam graphite monochromator. The patterns were recorded in the 2-theta (2θ) range from 2° to 80°, in steps of 0.02° and counting time 2 s per step.

3. Results and discussion

The quality and nature of carbon deposited on the aluminosilicate surfaces were examined by transmission electron microscopy (TEM) and scanning electron microscopy (SEM). The TEM bright-field images in Fig. 1 clearly show the development of hollow carbon nanotubes with tips attached to iron moieties embedded on the clay surfaces. The formation of hollow carbon tubes on clay surfaces is in accord with the synthesis of carbon nanotubes from the deposition of acetylene or other gaseous hydrocarbons at 700 °C over supported metal nanoparticles [13,14,22–24], while at lower temperatures (below 500 °C) almost solid carbon fibers are produced [24]. Besides carbon tubes, the formation of amorphous carbon surrounding the clay catalyst particles is also seen (Fig. 1a). The tubes exhibit various relative orientations and many are in close proximity. The average outer diameter is between 25 and 35 nm and their length is up to 10 μm. Many tubes bridge different clay platelets, some contain encapsulated opaque particles (dark spots), which are due to the transition metal catalyst [25,26], while others have their tips free of metallic particles (Fig. 1b). The rooting of the tubes in the catalytic sites on the clay surfaces is clearly seen in Fig. 1c. The ferruginous nanoparticles (dark spots), embedded on the clay platelets (of approximately 0.1 ìm), catalyze the decomposition of acetylene to form carbon nanotubes. A non-uniform nanotube growth is observed, that probably results from a non-uniform distribution of catalytic nanoparticles in the clay surfaces. This can happened because heating an Fe(III)-exchanged clay at 450 °C transform the interlayer iron cations to fine iron oxide particles which migrate to the outer surface in a random way [27]. The SEM image in Fig. 2 illustrates the clustering of the tubes at the clay surfaces in a worm like morphology. The combined TEM and SEM results point to a growth medium comprised of delaminated clay layers covered with carbon tubes or, otherwise, to the formation of a three dimensional network of clay layers decorated with carbon tubes. Fig. 3 represents a dynamic simulation of the clay–carbon nanotube composite created by using the experimental TEM and SEM results and a three-dimensional drawing and model-

(a)

Fig. 2. SEM image of clay–carbon nanotube composites.
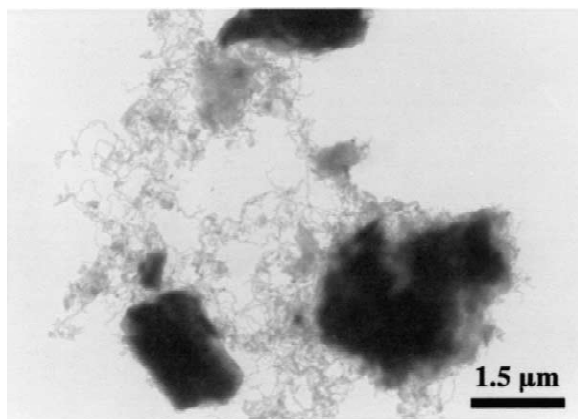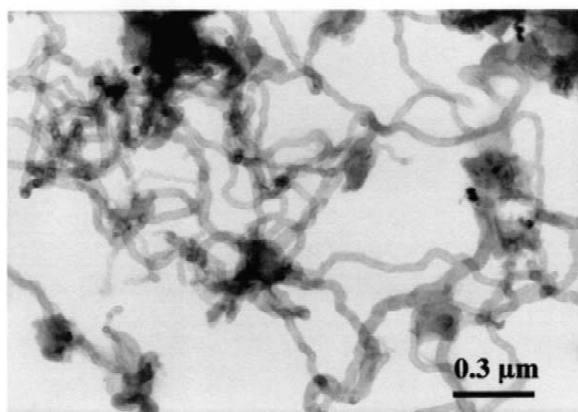
(b)
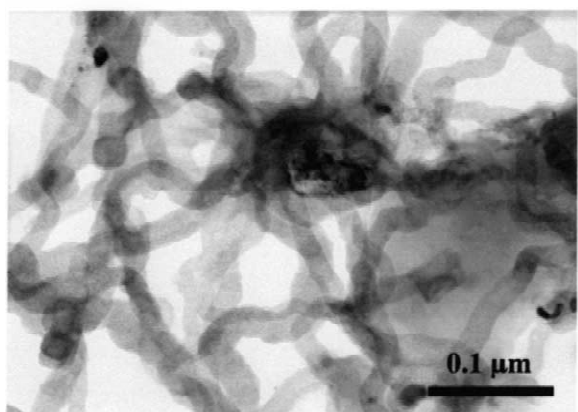
(c)

Fig. 1. TEM bright-field micrographs of a clay–carbon nanotube composite at different magnifications. Dark spots are iron catalytic centers attached to the clay surfaces.
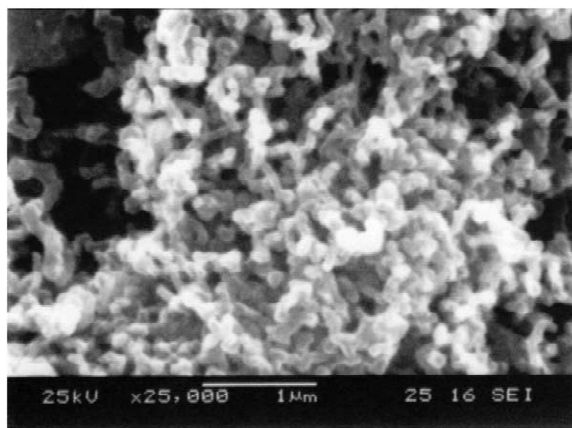
ing program (3D studio MAX Version 2.0). The image shows clearly the development of carbon tubes located at the clay platelets.

The clay–carbon nanotube composites exhibit macroscopic magnetic properties as evidenced by their attraction to a permanent hand magnet. In order to examine the nature of the iron centers and identify the magnetic iron phase we resorted to ^{57}Fe-Mössbauer spectroscopy. Fig. 4 shows the spectrum at 85 K of a clay–carbon nanotube composite (a) and that of an iron–clay sample heated at the same temperature and for the same time but only in argon gas instead of the acetylene–argon mixture (b). The profiles of the two spectra are quite different. It is obvious that the process of growing carbon nanotubes changes the nature of the initial iron sites and, therefore, their Mössbauer response. Thus, spectrum (b) consists of one magnetic component with parameters characteristic of α-Fe_2O_3 and one ferric doublet. On the other hand, spectrum (a) was adequately fitted with one magnetic sextet with $H = 24.7$ T, $IS_{Fe} = 0.32$ mm/s, $\Delta E_Q = -0.03$ mm/s. These values are characteristic of ferromagnetic cementite (Fe_3C) [28] and probably represent iron species attached to the two ends of the carbon nanotubes. Analogous Fe_3C phase was observed in $MgAl_2O_4$-matrix nanocomposite powders containing carbon-nanotubes and iron-based nanoparticles [29]. In addition, two paramagnetic doublets are necessary to fit the paramagnetic part with $IS_{Fe} = 1.16$ mm/s, $\Delta E_Q = 1.87$ mm/s and $IS_{Fe} = 1.24$ mm/s, $\Delta E_Q = 2.51$ mm/s. These centers arise likely from ferrous ions anchored to the silicate layer in the form of iron(II)–silicate species.

An important property of the clay–carbon tube composites is their ability to disperse in an aqueous medium of a cationic surfactant. Intercalation of the surfactant between the clay layers induces lamination or face-to-face stacking of the mineral layers. Similar intercalation and lamination was observed when the carbonaceous modified clay surfaces were exposed to triethylamine vapors. The X-ray
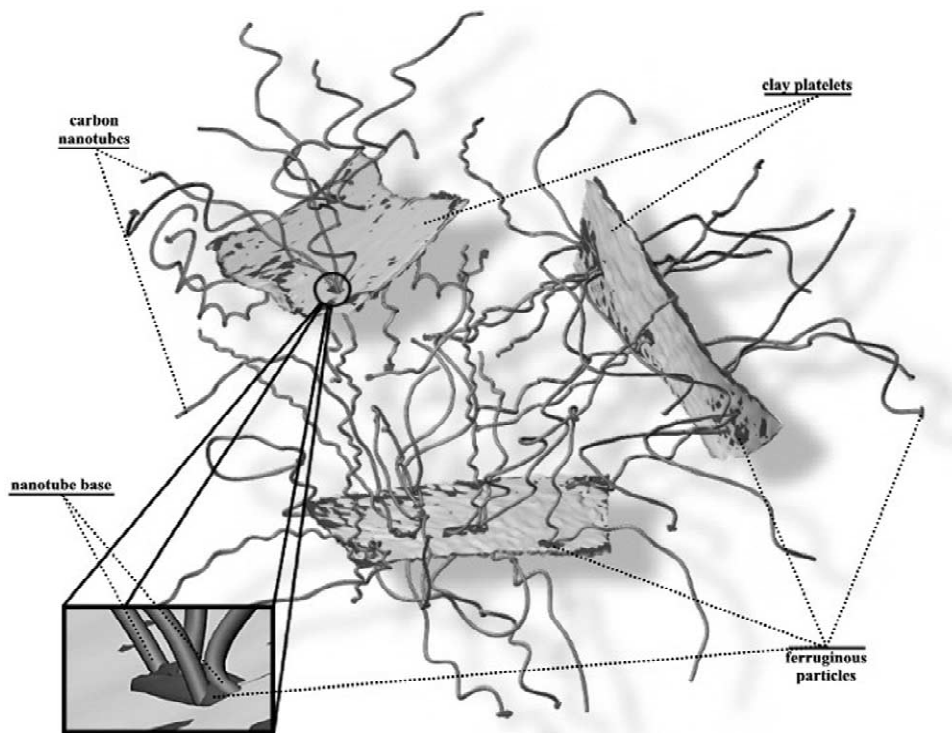
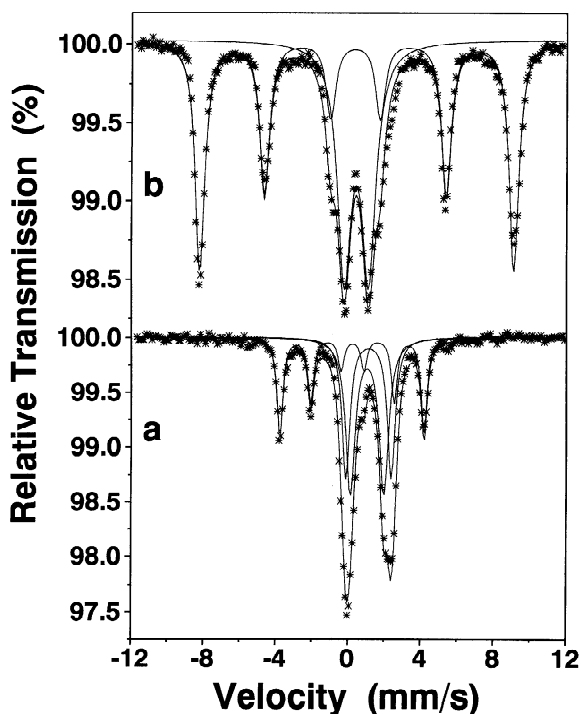Fig. 3. Schematic illustration of the clay–carbon nanotube composite.

Fig. 4. Mössbauer spectra at 85 K of an Fe(III)-exchanged montmorillonite treated: (a) with acetylene–argon at 700 °C for 45 min and (b) as in (a) but in argon only.

diffraction (XRD) results in Fig. 5 provide evidence for these features. The basal spacing (d_{001}) of 12.6 Å in pattern (a) refers to the original Fe(III)–clay system. Following formation of the tubes on the clay surfaces the lack of reflections in pattern (b) implies that the clay layers are delaminated. On the contrary, the large number of 001 reflections observed in pattern (c) indicates layer insertion of trimethylhexadecylammonium cations and a high degree of lamination of the clay–surfactant–carbon nanotube system. Similarly, protonation of the $(C_2H_5)_3N$ amine by the clay surfaces induces similar insertion as shown in pattern (d). These qualitative arguments are confirmed by intercalation experiments of either trimethylhexadecylammonium cationic surfactants or triethylamine vapors in a clay without carbon nanotubes (see dotted lines in Fig. 5c and d). The d_{001} values of composite materials in the presence and absence of carbon nanotubes are in good agreement proving that the clay in the clay–carbon nanotube composites retains its cation-exchange properties. The synthesis of such carbon nanotube–organoclay derivatives is of prime importance for the successful fabrication of composite polymer–organoclay–carbon tube materials. Organo-exchanged montmorillonite–carbon tube derivatives could interact with polymers to yield either intercalated or exfoliated hybrids [20]. Further work is in progress concerning the application of clay–carbon nanotubes for reinforcement of polymers.
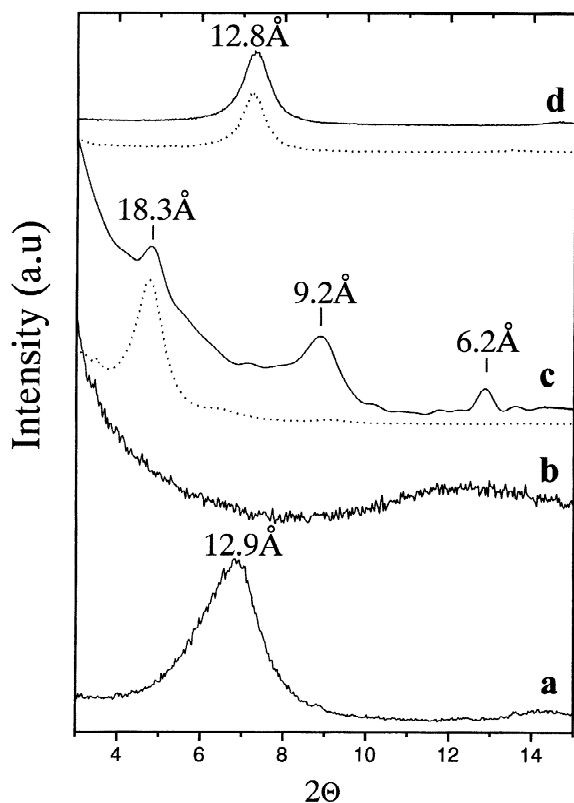
Fig. 5. Powder X-ray diffraction patterns of the original Fe(III)-clay (a) of a clay–carbon nanotube composite (b), of a clay–carbon nanotube sample after intercalation of trimethylhexadecylammonium cations (c) and triethyl amine (d). In the last two patterns the dotted lines represents XRD patterns after intercalation of a pristine clay sample with trimethylhexadecylammonium cations and triethylamine.

4. Conclusions

Carbon nanotubes can be synthesized on clay surfaces by the catalytic decomposition of acetylene on iron-exchanged montmorillonite. TEM micrographs show clearly the rooting of carbon nanotubes on the clay layers, the latter being in a delaminated state forming a three dimensional network. The tubes exhibit various relative orientations and many bridge different clay platelets. SEM images illustrate clustering of the tubes in a worm-like morphology. Mössbauer results point to the formation of ferromagnetic cementite (Fe_3C) as the main iron product attached to the ends of the tubes. The clay in the carbon-modified solid maintains its exchange properties making possible the generation of valuable carbon-nanotube–organoclay derivatives.

References

[1] Ajayan PM. Nanotubes from carbon. Chem Rev 1999;99(7):1787–99.

[2] Dresselhaus MS, Dresselhaus G, Eklund PC. Science of fullerenes and carbon nanotubes. New York: Academic Press, 1996.

[3] Terrones M, Hsu WK, Kroto HW, Walton DRM. Nanotubes: a revolution in materials science and electronics. In: Hirsch A, editor, Fullerenes and related structures, Topics in current chemistry, vol. 199, Heidelberg: Springer, 1998, pp. 189–234, chapter 6.

[4] Tans SJ, Verschueren AR, Dekker C. Room-temperature transistor based on a single carbon nanotube. Nature 1998;393(6680):49–52.

[5] Tans SJ, Devoret MH, Dai H, Thess A, Smalley RE, Geerlings LJ, Dekker C. Individual single-wall carbon nanotubes as quantum wires. Nature 1997;386(6624):474–7.

[6] Sinitsyn NI, Gulyaev YV, Torgashov GV, Chernozatonskii LA, Kosakovskaya ZY, Zakharchenko YF, Kiselev NA, Musatov AL, Zhbanov AI, Mevlyut ST, Glukhova OE. Thin films consisting of carbon nanotubes as a new material for emission electronics. Appl Surf Sci 1997;111:145–50.

[7] Collins PG, Avouris P. Nanotubes for electronics. Sci Am 2000;283(6):38–45.

[8] Calvert P. Nanotube composites: A recipe of strength. Nature 1999;399(6733):210–1.

[9] Wagner HD, Lourie O, Feldman Y, Tenne R. Stress-induced fragmentation of multiwall carbon nanotubes in a polymer matrix. Appl Phys Lett 1998;72(2):188–90.

[10] Dai HJ, Hafner JH, Rinzler AG, Colbert DT, Smalley RE. Nanotubes as nanoprobes in scanning probe microscopy. Nature 1996;384(6605):147–50.

[11] Britto PJ, Santhanam KSV, Ajayan PM. Carbon nanotube electrode for oxidation of dopamine. Bioelectrochem Bioenerg 1996;41(1):121–5.

[12] Dillon AC, Jones KM, Bekkedahl TA, Kiang CH, Bethune DS, Heben MJ. Storage of hydrogen in single-walled carbon nanotubes. Nature 1997;386(6623):377–9.

[13] Hernadi K, Fonseca A, Nagy JB, Bernaerts D, Fudala A, Lucas AA. Catalytic synthesis of carbon nanotubes using zeolite support. Zeolites 1996;17(5-6):416–23.

[14] Hernadi K, Fonseca A, Nagy JB, Bernaerts D, Lucas AA. Fe-catalyzed carbon nanotube formation. Carbon 1996;34(19):1249–57.

[15] Li WZ, Xie SS, Qian LX, Chang BH, Zou BS, Zhou WY, Zhao RA, Wang G. Large-scale synthesis of aligned carbon nanotubes. Science 1996;274(5293):1701–3.

[16] Dai H, Rinzler AG, Nikolaev P, Thess A, Colbert DT, Smalley RE. Single-wall nanotubes produced by metal-catalyzed disproportionation of carbon monoxide. Chem Phys Lett 1996;260(3/4):471–5.

[17] Tour JM, Cassell AM, Scrivens WA. Graphite electrodes containing nanometer sized metal particles and their use in

the synthesis of single-walled carbon nanotube composites. Chem Mater 1996;8(7):1545–9.

[18] Lagaly G. Introduction: from clay mineral–polymer interactions to clay mineral–polymer nanocomposites. Appl Clay Sci 1999;15(1/2):1–9.

[19] LeBaron PC, Wang Z, Pinnavaia TJ. Polymer-layered silicate nanocomposites: an overview. Appl Clay Sci 1999;15(1/2):11–29.

[20] Giannelis EP. Polymer layered silicate nanocomposites. Adv Mater 1996;8(1):29–35.

[21] Gournis D, Mantaka-Marketou A, Karakassides MA, Petridis D. Ionizing radiation-induced defects in smectite clays. Phys Chem Miner 2001;28(4):285–90.

[22] Colomer J-F, Piedigrosso P, Willems I, Journet C, Bernier P, Van Tendeloo G, Fonseca A, Nagy JB. Purification of catalytically produced multi-wall nanotubes. J Chem Soc Faraday Trans 1998;94(24):3753–8.

[23] Müller TE, Reid DG, Hsu WK, Hare JP, Kroto HW, Walton DRM. Synthesis of nanotubes via catalytic pyrolysis of acetylene: a SEM study. Carbon 1997;35(7):951–66.

[24] Cui S, Lu CZ, Qiao YL, Cui L. Large-scale preparation of carbon nanotubes by nickel catalyzed decomposition of methane at 600°C. Carbon 1999;37(12):2070–3.

[25] Saito Y, Yoshikawa T, Okuda M, Fujimoto N, Sumiyama K, Suzuki K, Kasuya A, Nishina Y. Carbon nanocapsules encaging metals and carbides. J Phys Chem Solids 1993;54(12):1849–60.

[26] Liu MG, Cowley JM. Encapsulation of manganese carbides within carbon nanotubes and nanoparticles. Carbon 1995;33(6):749–56.

[27] Bakas T, Moukarika A, Papaefthymiou V, Ladavos A, Gangas NH. Redox treatment of an Fe/Al pillared montmorillonite. A Mössbauer study. Clays Clay Miner 1994;42(5):634–42.

[28] Bi XX, Ganguly B, Huffman GP, Huggins FE, Endo M, Eklund PC. Nanocrystalline α-Fe, Fe_3C and Fe_7C_3 produced by CO_2 laser pyrolysis. J Mater Res 1993;8(7):1666–74.

[29] Coquay P, De Grave E, Vandenberghe RE, Dauwe C, Flahaut E, Laurent CH, Peigney A, Rousset A. Mössbauer spectroscopy study of $MgAl_2O_4$-matrix nanocomposite powders containing carbon nanotubes and iron-based nanoparticles. Acta Mater 2000;48(11):3015–23.